From Landmark Matching to Shape and Open Curve Matching: A Level Set Approach

W.-H. Liao[1], A. Khuu[1], M. Bergsneider[2], L. Vese[3], S.-C. Huang[1], and S. Osher[3]

[1] *Department of Biomathematics and Department of Molecular and Medical Pharmacology, UCLA, L.A., CA 90095*
[2] *Brain Injury Research Center, UCLA, L.A., CA 90095*
[3] *Department of Mathematics, UCLA, L.A., CA 90095*
All correspondences should be addressed to the first author at feuillet@ucla.edu

Abstract

In this paper, we present a new framework for warping shapes and open curves between two images. This method could also handle multiple pairs of shapes or curves. When implemented in 3-D, the same framework could be used to warp 3-D objects with minimal modification.

Our approach is to use the level set formulation to represent the shapes or curves to be matched. Using this representation, the problem becomes an energy minimization problem. Cost functions for warping overlapping, non-overlapping, and open curves are proposed. For overlapping shapes, a cost function based on minimizing the symmetric difference of the two shapes is used. This cost function is then generalized to deal with non-overlapping shapes as well. For warping open curves, we are inspired by the idea of geodesic active contours. A similar approach, which we will refer to as geodesic curve matching, is proposed. Euler-Lagrange equations are applied and gradient descent is used to solve the corresponding partial differential equations.

1. Introduction

Object warping is a challenging problem which deals with how to find a diffeomorphic transformation that match one object to the other. It is an important issue in computer vision and pattern recognition as well as many other scientific fields. Recently, image warping has also been an active research area in biomedicine to meet the challenges of representing and comparing different biological structures or images of different modalities. Several strategies of non-rigid warping algorithms have been proposed in the past decade.

Lots of efforts have also been made to represent shapes and objects mathematically and to compare them by rigorously defining and computing diffeomorphism and distance metric. For this beautiful subject, we refer the readers to [1-4].

One of the most popular techniques of non-rigid image warping is the landmark-based matching. The strategy of this method is to first identify user-defined landmarks that need to be matched. By interpolating the discrete matching of the landmarks, one tries to obtain a dense diffeomorphism for the whole image. This has been a very popular tool especially in creating special visual effects. For more details on landmark matching, we refer the reader to [5-7].

Another rapidly developing technique in image warping is the non-rigid dense matching. Most of these methods are based on the calculus of variations and partial differential equations. They start from forming a cost function that is minimized when the objects are matched. In order to ensure smooth matching, a regularizing term on the deformation field is often added. Dense matching could be used when landmarks are not available or when the information given by landmarks is not enough to provide accurate matching or to describe the characteristics of the objects. We will incorporate the technique of calculus of variations and extend the landmark matching to shape and open curve matching.

2. Background

In this section, we will provide a general overview of the setting for dense matching. We will use 2-D images for presentation but everything can be generalized to 3-D. We will follow the notations in [8], and thus we refer to this paper for more detailed description.

The terms template and study are often used to denote the images to be matched. Let us denote the template image as $T(x)$ and the study image as $S(x)$ which are images on the spatial domain $\Omega \subset R^2$. The problem of image warping is to find a displacement field $u(x)$ at each point x such that a properly defined distance measure, which will be denoted by $D(T,S,u)$, between the deformed template and the study is minimized. The displacement field is a vector field such that given any displacement field u the deformed template is given by $T(x\text{-}u)$. The term displacement is used because it can be viewed as how a point in the template is moved away from its original location. The most common way to define the measure between the deformed template and the study image is just the L^2 norm

$$D(T,S,u) = \frac{1}{2}\int_{\Omega} |\, T(x-u) - S(x)\,|^2 \, dx. \qquad (1)$$

Gradient descent of the corresponding Euler-Lagrange equation is often used to minimize this distance measure, and an artificial time t has to be introduced in order to solve for the displacement field. Thus we will denote the displacement u by $u(x,t)$ to avoid confusion. In the case of L^2 norm, the gradient decent partial differential equation is simply

$$\frac{\partial u(x,t)}{\partial t} = f(x,u(x,t))$$
$$f(x,u) = [T(x-u) - S(x)]\ \nabla T\ |_{x-u}\ . \quad (2)$$

The function $f(x,u(x,t))$ (up to a sign) is often called the force field or the body force, which describes the derivative of the distance measure with respect to the displacement field u. The term force field (body force) is used because this derivative could be viewed as the force that drives the deforming of the template.

Unfortunately this problem is known to be ill posed. One way to overcome this difficulty is to add another regularizer $R(u)$ on u to ensure smooth deformation. Thus, instead of minimizing $D(T,S,u)$, we now minimize the following new cost function

$$\min_u C(T,S,u) = \min_u (D(T,S,u) + \alpha R(u)). \quad (3)$$

Here α is the weight of the regularization. If we use a larger value we restrict the magnitude of deformation while a smaller value could yield a non-diffeomorphic transformation. In the next section, we will review several ways of regularization on the displacement field.

3. Previous Work

How to properly constrain the deformation depends on the nature of the matching. Several models for the regularization have been proposed and this is still an active field for research. All these models are based on different assumptions or analogies in physics. Yet in some sense, they all try to penalize large or oscillatory deformations that are not diffeomorphic. In this paper, we will describe some of the most well known models as well as the one we are going to adopt.

3.1. Hyper-elastic Registration

In hyper-elastic matching [9, 10], the authors tried to draw analogy between image warping and deforming elastic plates. Under the assumption of linear elasticity, which holds for relatively small displacement field only, we arrive at the following equation that should hold at equilibrium

$$\mu \Delta u(x,t) + (\mu + \lambda)\nabla(\nabla \cdot u(x,t)) = f(x,u(x,t)). \quad (4)$$

Here μ and λ are the *Lame* constants. Due to this linear elasticity assumption, large-magnitude displacements are severely penalized and thus hyper-elastic model is not suitable for problems in which large deformation and highly nonlinear deformation is needed.

3.2. Viscous Fluid Registration

The viscous fluid matching was first proposed by Christensen in [8]; thus for a detailed description of this model, we refer the reader to this paper and the references therein. To summarize, images are thought of being embedded in fluid flowing in accordance with the fluid-dynamic Navier-Stokes equations. The advantage of this method is that it allows large-magnitude deformations since stress constraining the deformation relaxes over time. Automatic re-gridding was also used in this method to prevent the local Jacobian from being too close to zero. The distance measure used in this model is the L^2 distance between $T(x\text{-}u)$ and $S(x)$ (though the name Gaussian sensor model was used). The disadvantage of this method is the relatively large computation load.

The partial differential equation that describes the deformation of the template could be written in the following form

$$\mu \Delta v(x,t) + (\mu + \lambda)\nabla(\nabla \cdot v(x,t)) = f(x,u(x,t)). \quad (5)$$

Here v is the velocity field and is related to the displacement field u in the following way

$$v(x,t) = u_t(x,t) + \nabla u(x,t) v(x,t)\ . \quad (6)$$

For more details on how to implement this method, please refer to [8, 11, 12].

3.3. Regularization proposed by Horn and Schunck

A third regularization, which we adopt in this paper, was originally used to regularize the velocity field in the optical flow problem (see, for example, chapter 5 in [13]). This regularizer was first proposed by Horn and Schunck in [14] by adding the following penalty on the velocity field v

$$R(v) = \frac{1}{2}\sum_{j=1}^{d} || \nabla v_j ||_{L^2}^2\ . \quad (7)$$

This penalty term is well known to smooth isotropically across the discontinuities. Thus, it is not suitable to regularize optical flow since discontinuities in the velocity field often exist on the boundary of moving objects. However, it is suitable for regularization in image warping where smooth deformation fields are expected.

The same regularizing term for image warping was proposed in [15] and the term fast diffusion registration was used.

In this paper, we will follow [15] and use this regularization for our shape and open curve matching problem. One advantage of this regularizer is that by employing the gradient descent to solve the corresponding Euler-Lagrange equation, we obtain an inhomogeneous heat equation

$$\frac{\partial u(x,t)}{\partial t} = f(x,u(x,t)) + \alpha \Delta u(x,t). \qquad (8)$$

Thus, the equations are decoupled for different components of u

$$\frac{\partial u_i(x,t)}{\partial t} = f_i(x,u(x,t)) + \alpha \Delta u_i(x,t). \qquad (8')$$

Moreover, this inhomogeneous heat equation allows fast computation via the operator splitting method (see implementation and results section).

4. Theory

In this paper, we try to generalize the landmark matching problem by replacing the finite pairs of landmarks to be matched by finite pairs of shapes or curves. We turn to the idea of level set method for ways of representing shapes and curves. The level set method was first proposed in [16] and has been proven to be a powerful tool in front tracking as well as many other applications. For an overview on level set method, we refer the readers to [17] and the references therein.

4.1. Shape matching

Let us start with shape matching. A shape could be represented by a level set function with the boundary of the shape being the zero level curve of the level set function (positive value inside the shape and negative outside). Throughout this paper we will use the following notation (see figure 1 (a)). The shapes in the template image will be denoted by the level set functions $\varphi_1, \varphi_2, \ldots, \varphi_n$ and the corresponding shapes in the study image by $\phi_1, \phi_2, \ldots, \phi_n$. Here n is the total number of pairs of shapes to be matched.

4.1.1. One Pair of Overlapping Shapes. Let us start from the simplest case of shape matching with only one pair of shapes (and thus we drop the subscript on the level set functions). In the template image, we have a shape represented by φ and a second shape in the study image by ϕ and our task is to find a displacement field that maps φ to ϕ.

In order to derive a suitable distance measure that is always non-negative and only takes the value zero when the two level set functions match, we borrowed the idea in [18]. In short, we try to minimize the symmetric difference of the two level set functions (the sum of the two areas denoted by $\varphi>0$, $\phi<0$ and $\varphi<0$, $\phi>0$ in figure 1 (b). We thus derive the following distance measure, which we will refer to as the overlapping distance measure

$$D(T,S,u) = \int_\Omega H(\phi(x))[1-H(\varphi(x-u))]\,dx + \int_\Omega H(\varphi(x-u))[1-H(\phi(x))]\,dx. \qquad (9)$$

The force field of this distance measure is

$$f(x,u) = [1-2H(\phi(x))]\delta(\varphi(x-u))\ \nabla\varphi|_{x-u}. \qquad (10)$$

Here H and δ are the Heaviside and the delta function.

4.1.2. One Pair of Non-overlapping Shapes. The above distance measure (Equation 9) does not work for non-overlapping shapes. The reason is that by minimizing the distance measure, φ will simply shrink to a point and the cost function will reach a local minimum. To overcome this we have to modify the distance measure so that it still works for non-overlapping shapes. The solution we propose is that, instead of integrating 1 in the area of the symmetric difference of the two level sets, we now integrate with respect to the level set function. To be more precise, in figure 1 (b) we integrate $-\phi$ in the area denoted by $\varphi>0$, $\phi<0$, and integrate $-\varphi$ in the area denoted by $\varphi<0$, $\phi>0$. To make this work, we now have to initialize the level set functions to be the signed distance function to their zero level sets. It is easy to see that the distance measure defined in this way, which we will refer to as the non-overlapping distance measure, is also non-negative and takes the value zero only when the two shapes match

$$D(T,S,u) = \int_\Omega -\varphi(x-u)\{H(\phi(x))[1-H(\varphi(x-u))]\}dx + \int_\Omega -\phi(x)\{H(\varphi(x-u))[1-H(\phi(x))]\}dx. \qquad (11)$$

In this case the force field is given by

$$f(x,u) = -\{H(\phi(x))[1-H(\varphi(x-u)) - \varphi(x-u)\delta(\varphi(x-u))] + [1-H(\phi(x))]\phi(x)\delta(\varphi(x-u))\}\nabla\varphi|_{x-u}. \qquad (12)$$

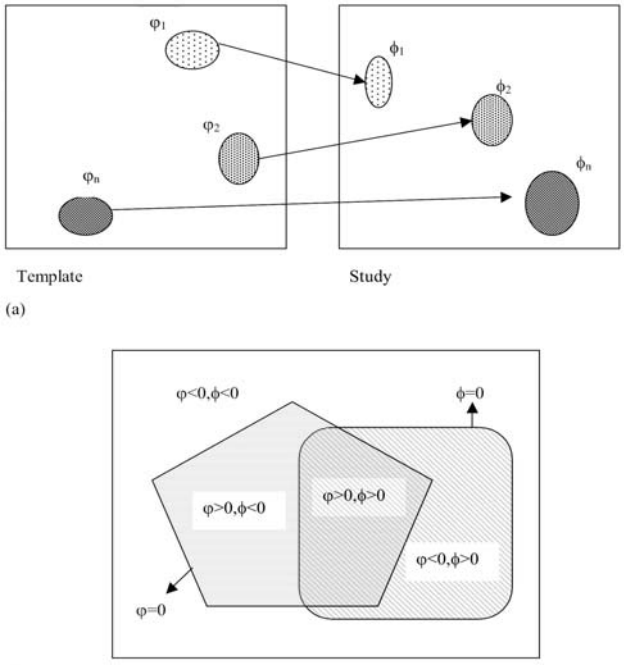

Figure 1. (a): Illustration of a general shape matching problem where multiple shapes represented by level set functions φ_i in the template need to be matched to ϕ_i in the study. (b): Illustration of four sub-regions divided by the level set functions, when the shapes in the template and study have overlap in space.

4.1.3. Matching Multiple Pairs of Shapes. The above formulation could be easily generalized to multiple pairs of shapes by combining distance measures. For example, the distance measure for matching multiple pairs of non-overlapping shapes is

$$D(T,S,u) =$$

$$\sum_{i=1}^{n}\int_{\Omega} -\varphi_i(x-u)\{H(\phi_i(x))\ [1-H(\varphi_i(x-u))]\}dx$$

$$+\sum_{i=1}^{n}\int_{\Omega} -\phi_i(x)\{H(\varphi_i(x-u))\ [1-H(\phi_i(x))]\}dx. \qquad (13)$$

4.2. Geodesic Open Curve Matching

Now we will turn to the more interesting problem of matching open curves by level set functions. As before we will focus on only one pair of open curves, as matching multiple pairs is just a direct extension. Our task is then to find a deformation field that maps an open curve C in the template to another open curve C' in the study.

It has been well known that one of the disadvantages of level set approach is one level set function can not represent an open curve. Several remedies have been introduced. In this paper, we will follow the smart idea in [19] by appending a second level set function. Please refer to figure 2. In order to find a representation of open curve C, we extend C to a closed curve (represented by the zero level set of φ_1), and we further draw a second closed curve (represented by the zero level set of φ_2), which crosses the zero level set of φ_1 only at the two end points of C.

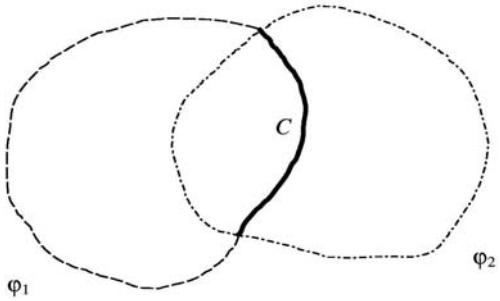

Figure 2. Illustration of how to represent an open curve using level set functions.

Then the open curve C could be written in the following way

$$C = \{x \mid \varphi_1(x) = 0 \ \text{and} \ \varphi_2(x) > 0\}. \qquad (14)$$

The open curve C' in the study image could also be represented by two level set functions ϕ_1 and ϕ_2. Let us further denote the distance functions of C and C' by $D_S(x)$ and $D_T(x)$. We then combine the idea of geodesic active contours [20] and the symmetric difference of two sets by minimizing the following distance measure

$$D(T,S,u) = \int_{\Omega} D_s(x)\delta(\varphi_1(x-u))\left|\nabla\varphi_1(x-u)\right| H(\varphi_2(x-u))dx$$

$$+\int_{\Omega} D_T(x-u)\delta(\phi_1(x))\left|\nabla\phi_1(x)\right| H(\phi_2(x))dx. \qquad (15)$$

This distance measure could be viewed as the sum of two line segment integrals with respect to the other curve's distance function, and thus is nonnegative and zero only when the two open curves are equal.

We will describe in detail how to obtain the Euler-Lagrange equation in this case. Note that all the derivations are in the sense of distributions. Let us first define $G(u)$ as the first part of the distance function

$$G(u) = \int_{\Omega} D_s(x)\delta(\varphi_1(x-u))\left|\nabla\varphi_1(x-u)\right| H(\varphi_2(x-u))dx. \qquad (16)$$

We want to compute the derivative of G along a test function v

$$\lim_{\varepsilon\to 0}\frac{G(u+\varepsilon v)-G(u)}{\varepsilon}. \qquad (17)$$

We first introduce the following notations

$$\delta_1 = \delta(\varphi_1(x-u)), H_2 = H(\varphi_2(x-u)), \delta_2 = \delta(\varphi_2(x-u))$$

By expanding the numerator in (17) up to first order, we get the following three terms

$$\int_{\Omega} D_s \delta_1' H_2 \left|\nabla\varphi_1(x-u)\right|\left[-\varepsilon \nabla\varphi_1 \mid_{x-u} v\right] dx \qquad (18)$$

$$\int_{\Omega} D_s \delta_1 H_2 \frac{\nabla\varphi_1(x-u)\nabla\left[-\varepsilon \nabla\varphi_1 \mid_{x-u} v\right]}{\left|\nabla\varphi_1(x-u)\right|} dx \qquad (19)$$

$$\int_{\Omega} D_s \delta_1 \delta_2 \left|\nabla\varphi_1(x-u)\right|\left[-\varepsilon \nabla\varphi_2 \mid_{x-u} v\right] dx \qquad (20)$$

Now we apply integration by parts on (19) and assume Neuman boundary conditions, we get

$$(19) = -\int_{\Omega} div(D_s \delta_1 H_2 \frac{\nabla\varphi_1(x-u)}{\left|\nabla\varphi_1(x-u)\right|})\left[-\varepsilon \nabla\varphi_1 \mid_{x-u} v\right] dx$$

$$= -(18) - \int_{\Omega} \delta_1 div(D_s H_2 \frac{\nabla\varphi_1(x-u)}{\left|\nabla\varphi_1(x-u)\right|})\left[-\varepsilon \nabla\varphi_1 \mid_{x-u} v\right] dx. \qquad (21)$$

Thus, term (18) is canceled in the numerator of (17) by negative (18) from the expansion of (19). Let us further work on the integrand of the remaining term in (21)

$$div\left[D_s H_2 \frac{\nabla\varphi_1(x-u)}{\left|\nabla\varphi_1(x-u)\right|}\right] =$$

$$\frac{\{ H_2 < \nabla D_s, \nabla\varphi_1 \mid_{x-u} > + D_s \delta_2 < \nabla\varphi_2 \mid_{x-u}, \nabla\varphi_1 \mid_{x-u} >\}}{\left|\nabla\varphi_1(x-u)\right|}$$

$$+ D_s H_2 div(\frac{\nabla\varphi_1(x-u)}{\left|\nabla\varphi_1(x-u)\right|}) . \qquad (22)$$

Now we could put everything together and obtain the following force field given by this distance measure

$$-\frac{\delta_1}{\left|\nabla\varphi_1(x-u)\right|}\{ H_2 < \nabla D_s, \nabla\varphi_1 \mid_{x-u} >$$

$$+ D_s \delta_2 < \nabla\varphi_2 \mid_{x-u}, \nabla\varphi_1 \mid_{x-u} >\} \nabla\varphi_1 \mid_{x-u}$$

$$-\delta_1 D_s H_2 div(\frac{\nabla\varphi_1(x-u)}{\left|\nabla\varphi_1(x-u)\right|})\nabla\varphi_1 \mid_{x-u}$$

$$+ D_s \delta_1 \delta_2 \left|\nabla\varphi_1(x-u)\right| \nabla\varphi_2 \mid_{x-u} + \delta(\phi_1)\left|\nabla\phi_1\right| H(\phi_2)\nabla D_T \mid_{x-u} \qquad (23)$$

We shall make a remark here that by combining distance measures, we can warp images in which multiple pairs of both shapes and open curves are to be matched.

5. Implementation

Finite difference method will be used to solve the gradient descent time-evolution partial differential equations. The equations that we are going to solve all have the form of inhomogeneous heat equations. Let us group everything other than the Laplacian operator together and write our PDE in the following way

$$\frac{\partial u(x,t)}{\partial t} = F(x, u(x,t)) + \alpha \Delta u(x,t) . \qquad (24)$$

One can solve this using fully explicit scheme but the disadvantage of the fully explicit scheme is that the step size Δt has to be very small. One remedy is to use a semi-implicit scheme and invoke the Additive Operator Splitting (AOS). The AOS scheme was first proposed in image processing by Weickert [21, 22] for efficiently solving non-linear diffusion filtering problem. The trick here is to replace the Laplacian operator on the right hand side at the current time step with the next time step. To be more precise, let the vector $u^n = (u^n_{0,0}, u^n_{0,1}, ..., u^n_{m-1,m-1})$ be a lexicographical ordering of the values of the displacement field at the grid points at time step *n* and A_l be the usual 3-point finite difference approximation operator of the second order derivative along the *l*-th space coordinate. We denote the finite difference approximation of $F(x, u(x,t))$ described above at the grid points at time step *n* by $F^n = (F^n_{0,0}, F^n_{0,1}, ..., F^n_{m-1,m-1})$. Then the semi-implicit scheme is

$$\frac{u^{n+1} - u^n}{\Delta t} = \alpha \sum_{l=1}^{d} A_l u^{n+1} + F^n , \qquad (25)$$

$$\text{or } u^{n+1} = \left(I - \Delta t\ \alpha \sum_{l=1}^{d} A_l \right)^{-1} \left(u^n + \Delta t\ F^n \right). \qquad (26)$$

This scheme could not be solved explicitly and involves inversion of a sparse matrix with five bands (in two-dimensional case). The trick of AOS is to replace the above problem by solving the following instead

$$u^{n+1} = \frac{1}{d} \sum_{l=1}^{d} \left(I - d\ \Delta t\ \alpha A_l \right)^{-1} \left(u^n + \Delta t\ F^n \right). \qquad (27)$$

This smart splitting has the same local truncation error as the original semi-implicit scheme and is of order one in time and order two in space. Moreover, it is unconditionally stable. By splitting the operator into a coordinate-by-coordinate fashion, we now only need to invert a tri-diagonal matrix along each coordinate and this allows an O(m^2) implementation by the Thomas algorithm. From our experience, a speed-up of at least a magnitude of 10 compared to the fully explicit scheme could be achieved by using the AOS scheme.

6. Results

In this paper, all the images are of size 128 by 128 pixels. The grid size is 0.1. The numerical approximations for calculating the Heaviside function and the delta function could be found in [23].

6.1. One pair of non-overlapping shapes

In the first experiment, we look at one pair of non-overlapping shapes. Figure 3 shows the template (a) and the study image (b). The shapes are constructed such that the inner rim in the study does not touch the outer rim in the template. The weight α used in this experiment is 0.04 and the time discretization *dt* is 0.1.

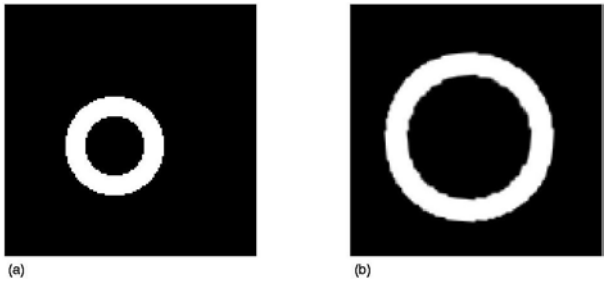

Figure 3. Illustration of a matching problem with two non-overlapping rings in the template (a) and the study (b).

1500 iterations are used to calculate the final displacement field. Figure 4 shows the final warped shape and the underlying grid deformation of the template.

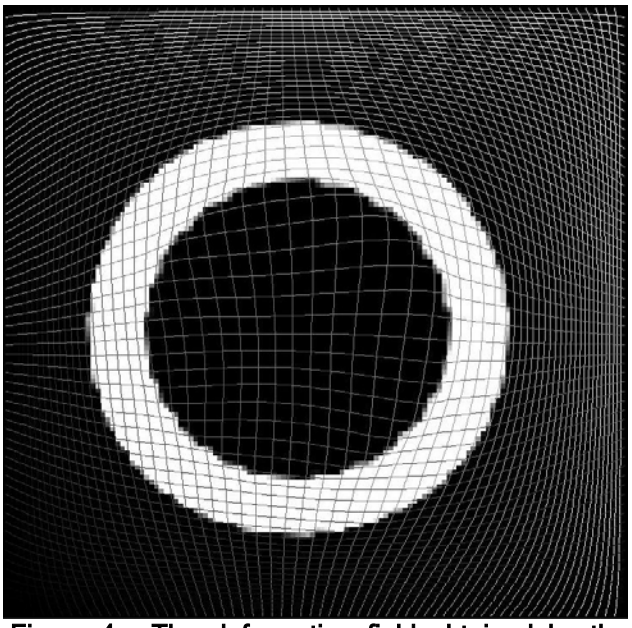

Figure 4. The deformation field obtained by the proposed method for matching figure 3 (a) to 3 (b).

6.2. One pair of open curves

In this experiment, we look at one pair of open curves. We extracted two arcs from two circles (different center and radius) as our open curves. Figure 5 shows the template (a) and the study image (b). The weight α used in this experiment is 0.015 and the time discretization *dt* is 0.04.

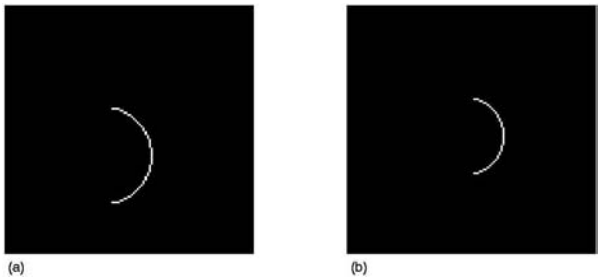

Figure 5. Illustration of a matching problem with two arcs in the template (a) and the study (b).

3000 iterations are used to calculate the final displacement field. Figure 6 shows the final warped open curve and the underlying grid deformation of the template.

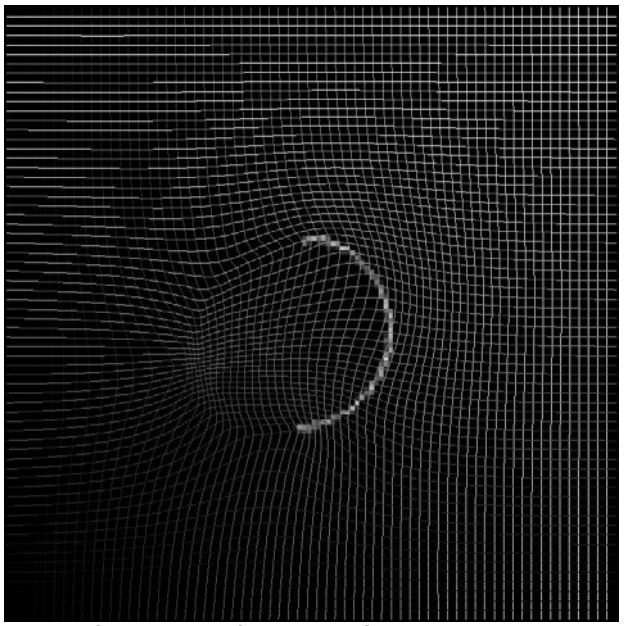

Figure 6. The deformation field obtained by the proposed method for matching figure 5 (a) to 5 (b).

6.3. Two pairs of non-overlapping shapes

This experiment is the most challenging case. Figure 7 (a) shows the template image. The study image, though not shown here, is visually identical to the final warped

template shown in figure 7 (f). The goal here is to match two pairs of non-overlapping circular shapes.

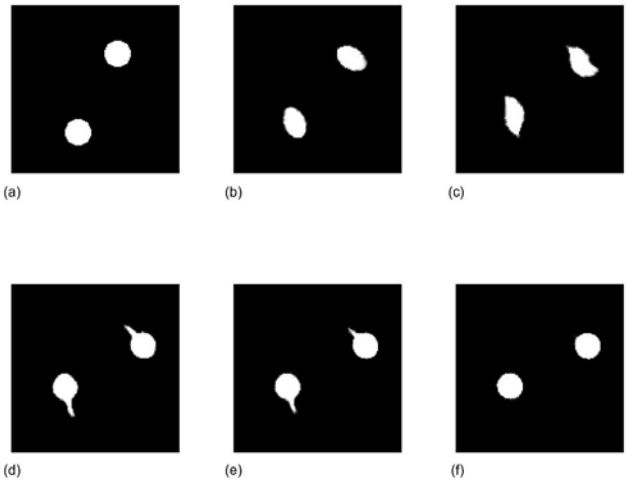

Figure 7. The intermediate shapes in the matching process in 6.3 at iteration 0 or template (a), 100 (b), 400 (c), 1000 (d), 1500 (e), and 6000 (f).

To avoid the shapes from shrinkage during the deforming process, we add a second constraint on the change of the area inside the shapes. We also constantly monitor the position of the deforming shapes in the template and we switch the distance measure to the overlapping distance measure once a substantial amount of overlapping is detected between the deforming shapes and the shapes in the study. In this experiment the non-overlapping distance measure is switched to the overlapping distance measure at iteration 500. The constraint on the change of area is also turned off at iteration 500. The weight α used is 0.01.

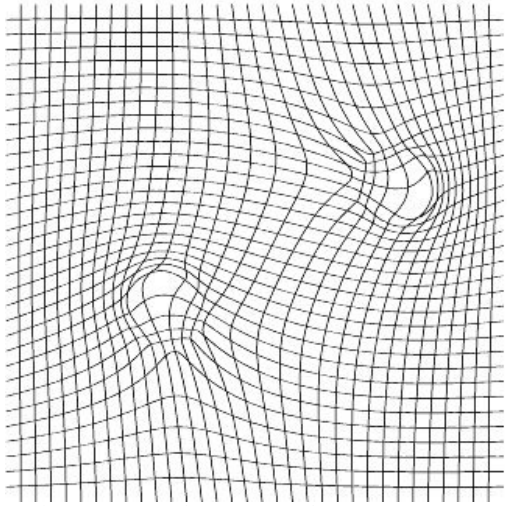

Figure 8. The deformation field obtained by the proposed method for matching figure 7 (a) to 7 (f).

Figure 7 shows the intermediate images in the deforming process at iteration 100 (b), 400 (c), 1000 (d), 1500 (e), and 6000 (f). The final deformation field corresponding to figure 7 (f) is shown in figure 8.

7. Discussions

In this section we will first explain why we have to switch the distance measures in experiment 6.3. We also will carefully re-examine the role of the level set functions. A new concept of re-initialization, which is different from the usual meaning of re-initialization, of the level set function will be proposed and discussed.

7.1. Distance measure switching in 6.3

For the experiment in 6.3, one may wonder why the original strategy with no switching of the distance measure does not work. This is a very subtle issue. It turns out that using non-overlapping distance measure alone in this experiment will generate slant shapes with tails and thus fail to match the two pairs of shapes. It can also be noted in the intermediate steps in figure 7 (d) and (e) in which long tails behind the shapes could be seen. A reasonable explanation is that the signed distance function property of the level set functions is gradually violated in the deforming process such that after some time the directional information in $\varphi(x\text{-}u)$ is almost lost and it is not suitable for further guiding the shapes toward the correct direction. That is why we have to use this two-step strategy of starting with one measure and switching to the other one once certain amount of overlapping is detected.

One could also argue that as we switch, we no longer care about the distance function property of the level set functions and thus all level set functions will do the job. In other words, the distance function property is only needed when the images do not overlap, and thus during this time directional information is provided by the level set functions. Once overlapping is detected, we can safely switch to the overlapping distance measure although now the level set function is no longer and far away from a distance function!!

7.2. Re-initialization of the distance function

In this section, we will discuss possible solutions to avoid switching the distance measure. A reasonable approach is to constantly adjust the level set function so that it is always close to the signed distance function with respect to the current displacement field.

Here we propose to re-initialize distance functions (φ in shape matching and D_T in open curve matching) once in several iterations in the following way. Let us use φ as an example. In the first term of the distance measure

proposed for the non-overlapping shapes in (11), we integrate $-\varphi(x-u)$ inside one piece of the symmetric difference. But we initialize $\varphi(x)$ to be the distance function when there is no displacement field at all ($u(x)=0$). Once we start updating u, we lose this nice property. In other words, ideally we would like the function $\varphi(x-u(x))$ to be always a distance function to its zero level curve for all displacement u

$$\left(\frac{\partial\varphi|_{x-u}}{\partial x_1}\right)^2+\left(\frac{\partial\varphi|_{x-u}}{\partial x_2}\right)^2=1. \quad (28)$$

This is a Hamilton-Jacobi equation in the form

$$a(u)\left(\frac{\partial\varphi}{\partial x_1}\right)^2+b(u)\frac{\partial\varphi}{\partial x_1}\frac{\partial\varphi}{\partial x_2}+c(u)\left(\frac{\partial\varphi}{\partial x_2}\right)^2=1. \quad (29)$$

Here a, b, and c are functions of u.

In short, the procedure of re-initializing includes fixing the zero level set and updating all the other values with respect to the current displacement field by solving (29), which for example, could be solved by the method in [24]. Numerical results will be reported in the future.

8. Conclusion

In this paper, we propose the problem of shape and open curve matching that can be viewed as a natural extension of the landmark-based matching problem. We solve this problem by incorporating level set method along with the calculus of variations and partial differential equations. Our numerical experiments show very promising results.

9. References

[1]L. Younes, "A distance for elastic matching in object recognition," *Comptes Rendus De L Academie Des Sciences Serie I-Mathematique*, vol. 322, pp. 197-202, 1996.

[2]L. Younes, "Computable elastic distances between shapes," *Siam Journal on Applied Mathematics*, vol. 58, pp. 565-586, 1998.

[3]L. Younes, "Optimal matching between shapes via elastic deformations," *Image and Vision Computing*, vol. 17, pp. 381-389, 1999.

[4]M. I. Miller and L. Younes, "Group actions, homeomorphisms, and matching: A general framework," *International Journal of Computer Vision*, vol. 41, pp. 61-84, 2001.

[5]F. L. Bookstein, *Morphometric tools for landmark data : geometry and biology*, 1st pbk. ed. Cambridge England ; New York: Cambridge University Press, 1997.

[6]F. L. Bookstein, "Principal warps: thin-plate splines and the decomposition of deformations," *IEEE Transactions on Pattern Analysis and Machine Intelligence*, vol. 11, pp. 567-85, 1989.

[7]S. C. Joshi and M. I. Miller, "Landmark matching via large deformation diffeomorphisms," *Ieee Transactions on Image Processing*, vol. 9, pp. 1357-1370, 2000.

[8]G. E. Christensen, R. D. Rabbitt, and M. I. Miller, "Deformable templates using large deformation kinematics," *IEEE Transactions on Image Processing*, vol. 5, pp. 1435-47, 1996.

[9]R. Dann, J. Hoford, S. Kovacic, M. Reivich, and R. Bajcsy, "Evaluation of Elastic Matching System for Anatomic (Ct, Mr) and Functional (Pet) Cerebral Images," *Journal of Computer Assisted Tomography*, vol. 13, pp. 603-611, 1989.

[10]R. Bajcsy and S. Kovacic, "Multiresolution Elastic Matching," *Computer Vision Graphics and Image Processing*, vol. 46, pp. 1-21, 1989.

[11]G. E. Christensen, R. D. Rabbitt, and M. I. Miller, "3D brain mapping using a deformable neuroanatomy," 1994.

[12]G. E. Christensen, S. C. Joshi, and M. I. Miller, "Volumetric transformation of brain anatomy," *IEEE Transactions on Medical Imaging*, vol. 16, pp. 864-77, 1997.

[13]G. Aubert and P. Kornprobst, *Mathematical problems in image processing : partial differential equations and the calculus of variations*. New York: Springer, 2001.

[14]B. K. P. Horn and B. G. Schunck, "Determining Optical-Flow," *Artificial Intelligence*, vol. 17, pp. 185-203, 1981.

[15]B. Fischer and J. Modersitzki, "Fast Diffusion Registration," *Institute of Mathematics, Medical University of Lubeck*, Preprint A-01-18, 2001.

[16]S. Osher and J. A. Sethian, "Fronts Propagating with Curvature-Dependent Speed - Algorithms Based on Hamilton-Jacobi Formulations," *Journal of Computational Physics*, vol. 79, pp. 12-49, 1988.

[17]S. Osher and R. P. Fedkiw, "Level set methods: An overview and some recent results," *Journal of Computational Physics*, vol. 169, pp. 463-502, 2001.

[18]R. T. Whitaker, "A level-set approach to image blending," *IEEE Transactions on Image Processing*, vol. 9, pp. 1849-61, 2000.

[19]P. Smereka, "Spiral crystal growth," *Physica D*, vol. 138, pp. 282-301, 2000.

[20]V. Caselles, R. Kimmel, and G. Sapiro, "Geodesic active contours," *International Journal of Computer Vision*, vol. 22, pp. 61-79, 1997.

[21]J. Weickert, "Recursive separable schemes for nonlinear diffusion filters," 1997.

[22]J. Weickert, B. M. T. H. Romeny, and M. A. Viergever, "Efficient and reliable schemes for nonlinear diffusion filtering," *IEEE Transactions on Image Processing*, vol. 7, pp. 398-410, 1998.

[23]T. F. Chan and L. A. Vese, "Active contours without edges," *Ieee Transactions on Image Processing*, vol. 10, pp. 266-277, 2001.

[24]Y. H. Tsai, L. T. Cheng, S. Osher, and H. K. Zhao, "Fast Sweeping Algorithms for a Class of Hamilton-Jacobi Equations," *UCLA CAM Report*, vol. 01-27, 2001.